NORMAL COORDINATE ANALYSIS OF INFRARED AND RAMAN SPECTRA OF *SYNDIOTACTIC* POLY(METHYL METHACRYLATE)

Jiří Dybal

Institute of Macromolecular Chemistry,
Czechoslovak Academy of Sciences, 162 06 Prague 6

Received December 29, 1990
Accepted February 4, 1991

Infrared and Raman spectra of crystalline *syndiotactic* poly(methyl methacrylate) have been analyzed by normal coordinate calculations, using a combined valence force field transferred from branched hydrocarbons and from methyl acetate. Calculations have been done for a single chain all-*trans* backbone structure of *syndiotactic* poly(methyl methacrylate) with parallel and antiparallel side-group orientations. The infrared and Raman bands observed can be satisfactorily interpreted on the basis of the calculated potential energy distributions. The best agreement between the calculated and experimental spectra has been found for the alternate *cis* and *trans* mutual orientations of the C=O and C—CH_3 bonds in subsequent monomeric units.

Results of infrared and Raman spectroscopic studies of *syndiotactic* poly(methyl methacrylate) (*s*-PMMA) have been presented in several papers[1-9]. Isotopic derivatives of *s*-PMMA were used in the interpretation of the methyl and methylene stretching and bending vibrations[1-3]. The temperature dependent bands in the infrared spectra of *s*-PMMA in bulk and in solution were tentatively assigned to various skeletal and side-group conformations[4-6]. Characteristic crystalline bands were determined[7-9] in the infrared spectra of partially crystalline *s*-PMMA samples obtained by the solvent induced crystallization[7,10,11]. However, the infrared and Raman spectra of *s*-PMMA have not been fully interpreted yet.

In a recent paper[12], a normal-mode analysis was used for studying the vibrational spectra of isotactic PMMA. On the basis of the potential energy distributions, infrared and Raman bands over the entire spectral region could be satisfactorily interpreted and a comparison of observed infrared and Raman bands with calculated frequencies supported the 10/1 helical conformation of crystalline *isotactic* PMMA. In this paper we present additional experimental results (Raman spectra) and a normal-mode analysis of the vibrational spectra and structure of crystalline *s*-PMMA.

X-ray diffraction and infrared dichroism of partially crystalline *s*-PMMA samples prepared by the solvent-induced crystallization indicate[7,10,11] that *s*-PMMA chains in the crystalline phase assume a helical conformation of large radius (a fourfold

helix with 74 monomeric units in a fibre period[11]). The results of NMR and infrared spectroscopy suggest the formation of double helices during the self-aggregation of *s*-PMMA in solution[9,13] and ^{13}C MAS NMR spectra[14] support an assumption[7] that double-helical structures also occur in crystalline *s*-PMMA. All these helical structures can be generated by *s*-PMMA chains with a nearly extended chain conformation of the backbone; according to the conformational energy calculations, the *tt* state of a racemic diad is the most favoured[15,16]. Therefore, in our normal-mode analysis based on the valence force constants refined for branched hydrocarbons[17] and for methyl acetate[18] the backbone structure of the *s*-PMMA chain was approximated by the *tt* staggered form. The calculations were performed using model structures of *s*-PMMA with both parallel and antiparallel orientations of ester side-groups.

EXPERIMENTAL

The tacticity of the *s*-PMMA sample studied was determined on the basis of proton NMR spectra; the content of *syndiotactic, heterotactic* and *isotactic* triads was 89·5, 8·5 and 2%, respectively. Partially crystalline *s*-PMMA was obtained by the solvent induced crystallization[7-11]. Samples were prepared by casting toluene and acetonitrile solutions on an aluminum foil followed by room temperature evaporation of the solvent under vacuum. Raman spectra were obtained with a Coderg LRDH 800 spectrometer. The spectra were excited by the 514·5 nm line of a Coherent CR-3 laser.

RESULTS AND DISCUSSION

The normal-mode calculations were done on a regular single chain all-*trans* structure of *s*-PMMA; the interchain forces in the double helical crystalline structure are weak compared to the intrachain ones and do not influence the frequencies significantly[12]. A structural repeat unit of the *s*-PMMA chain formed by two monomeric units is shown in Fig. 1. In the normal-mode calculations, the following bond lengths and bond angles were used: $CC^{\alpha} = C^{\alpha}C = C^{\alpha}C^{\beta} = 0{\cdot}153$ nm, $C^{\alpha}C^{*} = 0{\cdot}151$ nm, CH = 0·109 nm, C*O* = 0·121 nm, C*O = 0·134 nm, OC = 0·146 nm, $C^{\alpha}C^{*}O^{*} =$ = 127°, $C^{\alpha}C^{*}O = 122°$, C*OC = 117°, and the ester side-group was assumed to be in the planar conformation. The structural parameters of the ester group were taken from the *ab initio* optimization of the methyl acetate molecular geometry[19]. The main-chain torsional angles in the suggested structures of crystalline *s*-PMMA[10,11] are shifted from perfect staggering by 10 to 20° and according to the results of the conformational energy calculations of racemic PMMA diads, the skeletal bond angles are appreciably distorted relative to the tetrahedral value (the angle $C^{\alpha}CC^{\alpha}$ is ~124°). In the present calculations, however, we used empirical valence force fields derived for the branched hydrocarbons[17] and for methyl acetate[18] on the assumption that the corresponding bond angles are tetrahedral and that values used for

dihedral angles represent staggered or nearly staggered conformations. To ensure transferability of the force constants, these values for the structural parameters must therefore be used in the normal coordinate analysis[12].

Cartesian coordinates were calculated for the ideal all-*trans* backbone structure of the isolated *s*-PMMA chain. The local symmetry coordinates were constructed from the internal coordinates defined in the standard way[12]. According to the conformational energy calculations[16], there are two stable conformations of the side-groups in *s*-PMMA with *cis* and *trans* mutual orientations of the C=O and C—CH_3 bonds. Normal-mode calculations were performed for all three different structures of the extended *s*-PMMA chain defined by the stable conformations of the ester side-groups: *cis–cis*, *cis–trans*, *trans–trans*. The line group of the isolated *s*-PMMA chain with the side-chain conformations *cis–cis* or *trans–trans* is isomorphous to the point group C_{2v}. There are 86 optically active fundamental vibrations which are distributed among the symmetry species in the following manner: 25 A_1, 18 A_2, 18 B_1 and 25 B_2. All the normal modes are Raman active but the A_2 modes are infrared inactive. B_1 modes show parallel infrared dichroism, A_1 and B_2 modes show perpendicular infrared dichroism. There are no nontrivial symmetry elements associated with the line group for the *s*-PMMA zigzag chain with *cis–trans* side-chain conformations. Hence, the 86 optically active fundamental vibrations are both infrared and Raman active.

Raman spectra of the solid *s*-PMMA samples prepared by the room temperature evaporation of the solvent from toluene solution (partially crystalline[8]) and from

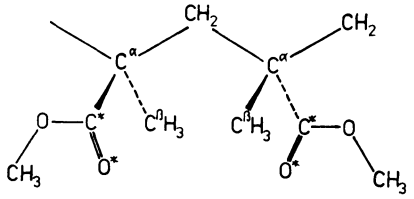

FIG. 1
Structural unit of *s*-PMMA

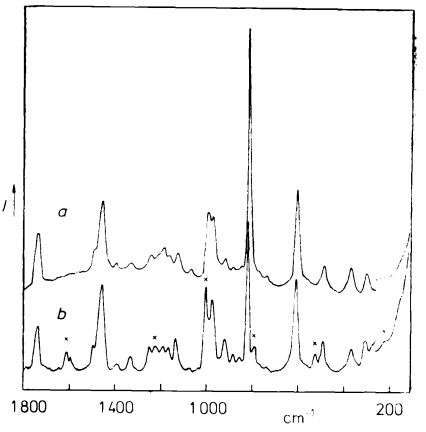

FIG. 2
Raman spectra of *s*-PMMA: *a* amorphous sample; *b* partially crystalline sample. × indicates peaks due to solvent

acetonitrile solution (amorphous[8]) are shown in Fig. 2. Similarly to the case of the infrared spectra[7-9], several differences can be observed between the Raman spectra of crystalline and amorphous *s*-PMMA, characteristic of a transition from unordered to ordered polymer. Some of the bands in the Raman spectrum of crystalline *s*-PMMA show frequency shifts and changes in intensity, e.g., the band at 910 cm^{-1} is shifted to 915 cm^{-1} and the intensity of the band at 877 cm^{-1} is appreciably higher in the spectrum of crystalline *s*-PMMA. In the spectrum of the crystalline form, a new weak band at 275 cm^{-1} appears that is not observed in the spectrum of the amorphous sample.

The observed Raman and infrared band frequencies of crystalline *s*-PMMA are listed in Table I. The experimental infrared frequencies are taken from our spectra published previously[8]. The infrared dichroism data given in Table I are taken from the papers of Nagai[1] and of Kusuyama et al.[7]. No polarization results are available for the Raman spectra because the measured samples have defined orientation.

According to the calculations of the conformational energies of the *s*-PMMA chain[16], three different stable conformational states defined by the ester side-group orientations are accessible to the racemic diad in the *tt* skeletal conformation. The lowest value of the total energy was found for the state with the *cis* positions of the C=O and C^{α}—C^{β} bonds in both monomeric units (*cis–cis*). The states with the *cis–trans* and *trans–trans* side-group orientations are higher in energy by 4·8 and 8·0 kJ mol^{-1}, respectively. Normal mode calculations have been performed for all the three structures.

Calculated frequencies of modes above 1 400 cm^{-1} corresponding to the localized vibrations differ for these structures by less than 1 cm^{-1}; significant differences appear in the range below 1 400 cm^{-1}. Calculated frequencies of selected vibrations of the extended *s*-PMMA chain with the *cis–cis*, *cis–trans* and *trans–trans* side-group orientations are listed in Table II and compared with the observed infrared and Raman band frequencies. In this table we list only modes above 200 cm^{-1} for which the calculated frequencies differ by 5 cm^{-1} or more. As can be seen from Table II, the calculated frequencies of the *cis–trans* state are in the best agreement with the bands observed. The average difference between the observed and calculated frequencies is 8·6 cm^{-1} for the *cis–trans* structure compared to 15·9 and 21·2 cm^{-1} for the *cis–cis* and *trans–trans* structure, respectively (the average difference for the *cis–trans* structure over the spectral range 1 800–200 cm^{-1} is 9·3 cm^{-1}). These results suggest that in the crystalline phase the ester side-groups of adjacent chemical repeat units have antiparallel orientation. Conformational energy calculations showing that the parallel *cis–cis* structure is more favourable were performed for the isolated racemic diad. However, *s*-PMMA chains in the crystalline state form a double helix[7,9,13,14] stabilized by intermolecular interactions not taken into account in the conformational calculations. Strong interactions of the ordered ester groups in crystalline *s*-PMMA are manifested in the splittings of the carbonyl

TABLE I

Observed and calculated frequencies (in cm^{-1}) of *syndiotactic* poly(methyl methacrylate)

Observed		Calculated	Potential energy distribution[b]
Infrared[a]	Raman		
3 026	3 030	3 025 A_1, B_1	OCH_3 as2(99)
2 999 π	3 002	3 002 A_2, B_1	OCH_3 as1(99)
		2 961 A_2, B_1	αCH as1(99)
2 952 σ	2 950	2 961 A_1, B_2	CH_3 as2(99)
		2 961 A_1, B_2	OCH_3 ss(99)
2 929	2 938	2 928 B_1, B_2	CH_2 ss(99)
	2 893	2 882 A_1, B_2	αCH_3 ss(100)
2 850 σ	2 845	2 855 A_1, A_2	CH_2 ss(100)
1 740, 1 731 σ	1 731	1 749 A_1, B_2	C=O s(83)
1 487 σ	1 487	1 476 A_1	CH_2 b(53), αCH_3 abl(31)
		1 467 A_2, B_1	αCH_3 ab2(85)
1 464		1 467 B_2	αCH_3 ab1(89)
		1 462 A_1	αCH_3 abl(57), CH_2 b(36)
1 450 π	1 451	1 457 A_2	CH_2 b(94)
		1 456 A_2, B_1	OCH_3 ab2(84), OCH_3 r2(16)
1 436 σ		1 446 A_1, B_2	OCH_3 sb(92)
		1 426 A_1, B_2	OCH_3 abl(69), OCH_3 r1(23)
1 403 σ		1 398 A_1	αCH_3 sb(48), CH_2 t(20)
1 382 σ	1 389	1 385 B_2	αCH_3 sb(84)
1 368 σ		1 355 A_1	αCH_3 sb(35) CH_2 t(18), CH_2 w(15), $C^{\alpha}C^{\beta}$ s(14)
1 340		1 350 B_2	CH_2 w(45), αCH_3 sb(21), $C^{\alpha}C^{*}$ s(10)
	1 326	1 318 B_1	CH_2 w(52), CC s2(46)
1 316		1 308 B_2	$C^{\alpha}C^{*}$ s(24), CH_2 w(18), C—O s(17), C=O ib(15)
1 278 σ		1 282 A_1	$C^{\alpha}C^{\beta}$ s(21), C—O s(15), C=O ib(14), CH_2 t(13), $C^{\alpha}C^{*}$ s(11)
1 242 σ	1 241	1 228 B_2	CC s1(40), αCH_3 r1(13), $C^{\alpha}CC^{\alpha}$ d(10)
	1 203	1 205 A_2	CC s2(42), αCH_3 r2(32)
		1 204 A_1	C—O s(21), OCH_3 r1(20), $C^{\alpha}C^{\beta}$ s(14)
1 193 σ		1 194 A_2	CH_2 t(96)
		1 192 B_2	OCH_3 r1(50), OCH_3 ab1(19)
	1 183	1 182 A_1	OCH_3 r1(32), O—C s(14), C=O ib(11)
1 171 π		1 178 B_1	CH_2 w(40), αCH_3 r2(21), CC s2(17)
1 149 σ	1 158	1 156 B_2	CC s1(29), C—O s(18), O—C s(17), αCH_3 r1(14)
1 122	1 126	1 128 A_2, B_1	OCH_3 r2(82), OCH_3ab2(16)
1 065 σ	1 064	1 047 A_1	O—C s(65), OCH_3 r1(13)
1 026 σ		1 036 B_2	O—C s(76), OCH_3 r1(10)
992 σ	987	1 023 A_1	αCH_3 r1(41), O—C s(16), $C^{\alpha}C^{\beta}$ s(16)
967 π	967	986 B_1	αCH_3 r2(29), CH_2 r(28), CC s2(17), C^{*} b2(12)

TABLE I
(*Continued*)

Observed		Calculated	Potential energy distribution[b]
Infrared[a]	Raman		
951		960 B_2	αCH_3 r1(54), CC s1(20), CH_2 r(12)
		929 A_2	αCH_3 r2(48), CC s2(46)
913 π	915	920 B_1	CH_2 r(43), αCH_3 r2(30), CC s2(17)
		912 A_1	$C^{\alpha}C^{\beta}$ s(33), αCH_3 r1(17)
863 σ	876	858 B_2	$C^{\alpha}C^{\beta}$ s(33), CH_2 r(24), C—O s(10)
828		811 B_2	$C^{\alpha}C^{\beta}$ s(17), C—O s(14), COC d(12)
810 σ	812	810 A_1	C—O s(18), COC d(15), O—C s(11), $C^{\alpha}C^{\beta}$ s(11), C=O ib(11)
		802 A_2	C=O ob(42), C* b2(18), CC s2(18), $C^{\alpha}CC^{\alpha}$ d(12)
747 π	736	758 B_1	C=O ob(67)
643	631	634 B_2	$C^{\alpha}C^{*}$ s(26), C=O ib(19), $CC^{\alpha}C$ d(17), C^{β} bl(13)
		615 A_2	$C^{\alpha}CC^{\alpha}$ d(42), C=O ob(28), C^{β} b2(19)
598	602	596 A_1	$C^{\alpha}C^{*}$ s(30), C=O ib(20), $CC^{\alpha}C$ d(12)
508, 486 σ	509, 484	492 A_1	CCO d(22), C* b1(17), C^{β} b1(17)
459		467 B_2	CCO d(25), $CC^{\alpha}C$ d(19), C* b1(18)
393	391	398 B_1	C^{β} b2(71), CH_2 r(11)
364	363	367 B_2	$CC^{\alpha}C$ d(24), COC d(18), C^{β} b1(17)
340		346 A_1	COC d(50), C=O ib(19), C* b1(13)
319		336 B_2	C=O ib(24), COC d(23), C* b1(22), $CC^{\alpha}C$ d(16)
	301	304 B_1	C* b2(47), C—O tor(23), C^{β} b2(12)
276	275	290 A_1	$CC^{\alpha}C$ d(40), C^{β} b1(17), COC d(12)
241	238	235 A_2	C^{β}b2(64), C—O tor(12)
220		231 B_2	C^{β} b1(38), $CC^{\alpha}C$ d(13), C* b1(11)
201		199 B_1	$C^{\alpha}C^{\beta}$ tor(74), C—O tor(15)
		197 A_2	$C^{\alpha}C^{\beta}$ tor(97)
		192 B_2	C* b1(49), CCO d(39)
		187 A_2	C—O tor(38), $C^{\alpha}C^{\beta}$ tor(26), $C^{\alpha}CC^{\alpha}$ d(14), O—C tor(11)
		168 B_1	C—O tor(40), O—C tor(27)
	153	166 A_1	CCO d(42), C* b1(37)
		130 A_2	O—C tor(79), C—O tor(10)
		125 B_1	O—C tor(69), C—O tor(24)
		81 A_2	C* b2(43), $C^{\alpha}C^{*}$ tor(19), $C^{\alpha}CC^{\alpha}$ d(13)
		62 B_1	$C^{\alpha}C^{*}$ tor(25), $C^{\alpha}C$ tor(25), CC^{α} tor(25)
		39 A_2	$C^{\alpha}C^{*}$ tor(77)
		35 B_1	$C^{\alpha}C^{*}$ tor(64)
		24 A_1	$C^{\alpha}C$ tor(47), CC^{α} tor(47)

bands in the infrared and Raman spectra[8,9]. The preference of structures with antiparallel orientations of the side-groups in crystalline *s*-PMMA is most likely due to cooperative intermolecular interactions of ester groups.

Our normal coordinate analysis of the spectra of crystalline *s*-PMMA is based on the model structure with all-*trans* backbone conformations and antiparallel esters. The calculated frequencies are listed in Table I together with the potential energy distributions (PED). The *s*-PMMA zigzag chain with parallel esters has the C_{2v} symmetry; the structure with antiparallel ester has the C_1 symmetry and all the modes belong to one type of symmetry species. However, this structure differs from the C_{2v} symmetry structure only by the rotation of one of the ester side-groups in the racemic diad. Therefore, the vibrational modes associated predominantly

TABLE II

Observed and calculated frequencies (in cm^{-1}) of selected vibrations of *syndiotactic* poly(methyl methacrylate)

Observed		Calculated[b]			Potential energy distribution[c]
Infrared[a]	Raman	I	II	III	
1 278 σ		1 296	1 282	1 245 A_1	CC s1(38), $C^{\alpha}CC^{\alpha}$ d(18), $C^{\alpha}C^{\beta}$ s(18) C^{β} b1(12)
1 242 σ	1 241	1 246	1 228	1 234 B_2	C—O s(41), CH_2 t(24), C=O ib(20)
1 149 σ	1 158	1 148	1 156	1 170 B_2	O—C s(18), C—O s(16), $C^{\alpha}C^{\beta}$ s(15), CH_2 r(14), C=O ib(12)
643		615	634	649 B_2	$C^{\alpha}C^{*}$ s(24), C=O ib(23), $CC^{\alpha}C$ d(16), C^{β} b1(15)
508, 486 σ	509, 484	458	492	473 A_1	$CC^{\alpha}C$ d(21), CCO d(18), CH_2 r(14), C^{*} b1(12)
364	363	380	367	359 B_2	COC d(39), C=O ib(17), C^{β} b1(11)

[a] Infrared bands: σ indicates electric vector perpendicular to the chain axis. [b] Calculated frequencies for the following side-group structures: *trans–trans* (I), *cis–trans* (II), *cis–cis* (III). [c] PED for the structure with parallel esters (*cis–cis*) is given (only contributions of 10% or greater are included): s stretch, b bend, ib in-plane-bend, d deformation, r rock, t twist.

←

[a] Infrared bands: π indicates electric vector along the chain axis, σ indicates electric vector perpendicular to the chain axis. [b] PED (only contributions of 10% or greater are included): s stretch, as antisymmetric stretch, ss symmetric stretch, b bend, ab antisymmetric bend, sb symmetric bend, ib in-plane bend, ob out-of-plane bend, d deformation, r rock, w wag, t twist, tor torsion.

with motions of atoms not belonging to ester groups practically preserve the symmetry behaviour of the parallel structure (C_{2v} symmetry). In Table I, symmetry types of the corresponding vibrations of the *s*-PMMA chain with parallel esters (*cis–cis*) are given for all calculated frequencies. The calculated frequencies and PEDs of several pairs of localized vibrations are practically identical. Therefore, in Table I such modes are given in one line where the two symbols of the corresponding symmetry species are included.

Assignments of the observed bands to the calculated modes were made on the basis of extensive spectral studies of isotopic derivatives of *s*-PMMA[1-3] as well as the infrared dichroism data[1,7]. The proposed assignments were correlated with the results of our normal-mode analysis of *isotactic* PMMA[12].

As can be seen in Table I, the results of the normal-mode analysis suggest a reasonable interpretation of the observed bands in the C—H stretch region, from 3 100 to 2 800 cm^{-1}. The calculated PEDs are in a qualitative agreement with the results of studies of deuterated *s*-PMMA[1,2]. The observed splitting of the C=O stretch mode (1 740 and 1 731 cm^{-1}) can be explained by resonance transition dipole coupling interactions[9]. These interactions were not included in the present calculations of the isolated *s*-PMMA chain.

The region from 1 500 to 1 350 cm^{-1} contains symmetric and asymmetric bend modes of methyl and methylene groups. The infrared band at 1 340 cm^{-1} and the Raman band at 1 326 cm^{-1} correspond essentially to CH_2 wag modes.

Similarly to the case of *isotactic* PMMA[12], the region from 1 300 to 1 150 cm^{-1} consists of mixed modes that are highly coupled along the chain. Frequencies of the bands observed at 1 278 and 1 242 cm^{-1} are very sensitive to the side-chain orientations (Table II). The weak band found at 1 107 cm^{-1} in the infrared spectrum is not predicted by the normal-mode calculations. We suppose that this band belongs to a combination, probably $596(A_1) + 492(A_1)$. The localized OCH_3 rock 2 modes of *s*-PMMA are predicted at the same frequencies (1 128 cm^{-1}) as for *isotactic* PMMA[12]. The assignments of the observed bands in the 1 000–900 cm^{-1} region to the OCH_3 and αCH_3 rock vibrations[1-3] are essentially confirmed by the normal vibrational analysis. However, the calculated PEDs indicate large contributions from O—C stretch and skeletal C—C stretch vibrations.

The characteristic bands of the crystalline phase of *s*-PMMA observed at 863 cm^{-1} in the infrared spectrum and at 876 cm^{-1} in the Raman spectrum correspond to the $C^{\alpha}C^{\beta}$ stretch vibration interacting with the CH_2 rock vibration. These bands are due to a long sequence of *tt* skeletal conformations. Another band observed at 843 cm^{-1} corresponds to the same mode for a structure containing gauche conformations[8].

On the basis of the spectra of deuterated derivatives, the bands observed at 747 and 736 cm^{-1} in the infrared and Raman spectra, respectively, were assigned to

the CH_2 rock vibrations[1,2]. However, the calculated PED indicate that, similarly to the case of isotactic PMMA[12], these bands correspond predominantly to the C=O out-of-plane bend. The doublet observed near 500 cm^{-1} is not reproduced by the normal-mode calculations. It is probably due to a Fermi resonance between the fundamental mode calculated at 492 cm^{-1} (A_1) and the combination mode 346(A_1) + 166(A_1).

Vibrational modes in the low-frequency region below 400 cm^{-1} are highly mixed and are very difficult to assign. Vibrations in this region involve coupling of the backbone and ester group bends and torsions.

REFERENCES

1. Nagai H.: J. Appl. Polym. Sci. *7*, 1697 (1963).
2. Schneider B., Štokr J., Schmidt P., Mihailov P., Dirlikov S., Peeva N.: Polymer *20*, 705 (1979).
3. Dirlikov S. K., Koenig J. L.: Appl. Spectrosc. *33*, 555 (1979).
4. O'Reilly J. M., Mosher R. A.: Macromolecules *14*, 602 (1981).
5. Dybal J., Štokr J., Schneider B.: Polymer *24*, 971 (1983).
6. Dybal J., Schneider B., Mihailov M.: Collect. Czech. Chem. Commun. *49*, 2259 (1984).
7. Kusuyama H., Takase M., Higashihata Y., Tseng H. T., Chatani Y., Tadokoro H.: Polymer *23*, 1256 (1982).
8. Spěváček J., Schneider B., Dybal J., Štokr J., Baldrian J., Pelzbauer Z.: J. Polym. Sci., Polym. Phys. Ed. *22*, 617 (1984).
9. Dybal J., Spěváček J., Schneider B.: J. Polym. Sci., Polym. Phys. Ed. *24*, 657 (1986).
10. Bosscher F., Brinke G. T., Challa G.: Macromolecules *15*, 1442, (1982).
11. Kusuyama H., Miyamoto N., Chatani Y., Tadokoro H.: Polym. Commun. *24*, 119 (1983).
12. Dybal J., Krimm S.: Macromolecules *23*, 1301 (1990).
13. Dybal J., Spěváček J.: Makromol. Chem. *189*, 2099 (1988).
14. Spěváček J., Schneider B., Straka J.: Macromolecules *23*, 3042 (1990).
15. Sundararajan P. R., Flory P. J.: J. Am. Chem. Soc. *96*, 5025 (1974).
16. Sundararajan P. R.: Macromolecules *19*, 415 (1986).
17. Snyder R. G., Schachtschneider J. H.: Spectrochim. Acta *21*, 169 (1965).
18. Dybal J., Krimm S.: J. Mol. Struct. *189*, 383 (1988).
19. Van Alsenoy C., Scarsdale J. N., Schäfer L.: J. Mol. Struct. *90*, 297 (1982).

Translation revised by L. Kopecká.